1521-0111/12/8206-1082–1093$25.00
MOLECULAR PHARMACOLOGY
Vol. 82, No. 6
78873/3804607

Mol Pharmacol 82:1082–1093, 2012

Xenobiotics and Loss of Cell Adhesion Drive Distinct Transcriptional Outcomes by Aryl Hydrocarbon Receptor Signaling[S]

Nan Hao, Kian Leong Lee, Sebastian G. B. Furness, Cecilia Bosdotter, Lorenz Poellinger, and Murray L. Whitelaw

School of Molecular and Biomedical Science (Biochemistry) and Australian Research Council Special Research Centre for the Molecular Genetics of Development, the University of Adelaide, Adelaide, South Australia, Australia (N.H., M.L.W.); Cancer Science Institute of Singapore, National University of Singapore, Singapore, Singapore (K.L.L., L.P.); Monash Institute of Pharmaceutical Sciences, Monash University, Victoria, Australia (S.G.B.F.); and Department of Cell and Molecular Biology, Karolinska Institutet, Stockholm, Sweden (C.B., L.P.)

Received March 22, 2012; accepted August 30, 2012

ABSTRACT

The aryl hydrocarbon receptor (AhR) is a signal-regulated transcription factor, which is canonically activated by the direct binding of xenobiotics. In addition, switching cells from adherent to suspension culture also activates the AhR, representing a nonxenobiotic, physiological activation of AhR signaling. Here, we show that the AhR is recruited to target gene enhancers in both ligand [isopropyl-2-(1,3-dithietane-2-ylidene)-2-[*N*-(4-methylthiazol-2-yl)carbamoyl]acetate (YH439)]-treated and suspension cells, suggesting a common mechanism of target gene induction between these two routes of AhR activation. However, gene expression profiles critically differ between xenobiotic- and suspension-activated AhR signaling. *Por* and *Cldnd1* were regulated predominantly by ligand treatments, whereas, in contrast, *ApoER2* and *Ganc* were regulated predominantly by the suspension condition. Classic xenobiotic-metabolizing AhR targets such as *Cyp1a1*, *Cyp1b1*, and *Nqo1* were regulated by both ligand and suspension conditions. Temporal expression patterns of AhR target genes were also found to vary, with examples of transient activation, transient repression, or sustained alterations in expression. Furthermore, sequence analysis coupled with chromatin immunoprecipitation assays and reporter gene analysis identified a functional xenobiotic response element (XRE) in the intron 1 of the mouse *Tiparp* gene, which was also bound by hypoxia-inducible factor-1α during hypoxia and features a concatemer of four XRE cores (GCGTG). Our data suggest that this XRE concatemer site concurrently regulates the expression of both the *Tiparp* gene and its *cis* antisense noncoding RNA after ligand- or suspension-induced AhR activation. This work provides novel insights into how AhR signaling drives different transcriptional programs via the ligand versus suspension modes of activation.

Introduction

The aryl hydrocarbon receptor (AhR) is a basic helix-loop-helix/Per-Arnt-Sim homology (bHLH/PAS) transcription factor, which provides an adaptive response to xenobiotic compounds. Structure-activity relationship analyses suggest that the ligand-binding pocket of AhR is promiscuous. Both polycyclic aromatic hydrocarbons and halogenated aromatic hydrocarbons (HAHs) are classic activators that bind to AhR with high affinity (Denison and Nagy, 2003), whereas other compounds such as omeprazole (Dzeletovic et al., 1997) and isopropyl-2-(1,3-dithietane-2-ylidene)-2-[*N*-(4-methylthiazol-2-yl)carbamoyl]acetate (YH439) (Lee et al., 1996) that fall outside aromatic classification have also been shown to activate the AhR, with YH439 functioning as an atypical AhR ligand (Whelan et al., 2010).

This work was supported by the Australian Research Council and National Health and the Medical Research Council of Australia, the Singapore National Research Foundation and the Singapore Ministry of Education under the Research Centre of Excellence Programme, and the Swedish Research Council, the Swedish Cancer Society, and the European Union (FP 7, SYSTEQ).

Article, publication date, and citation information can be found at http://molpharm.aspetjournals.org.

http://dx.doi.org/10.1124/mol.112.078873.

[S] The online version of this article (available at http://molpharm.aspetjournals.org) contains supplemental material.

ABBREVIATIONS: AhR, aryl hydrocarbon receptor; bHLH, basic helix-loop-helix; PAS, Per-Arnt-Sim homology; HAH, halogenated aromatic hydrocarbons; YH439, isopropyl-2-(1,3-dithietane-2-ylidene)-2-[*N*-(4-methylthiazol-2-yl)carbamoyl]acetate; Hsp90, heat shock protein 90; Arnt, aryl hydrocarbon receptor nuclear translocator; XRE, xenobiotic response elements; TCDD, 2,3,7,8-tetrachlorodibenzo-*p*-dioxin; pML, major late promotor; bp, base pair(s); PCR, polymerase chain reaction; m, mouse; HEK, human embryonic kidney; shRNA, short hairpin RNA; DMSO, dimethyl sulfoxide; qRT, quantitative real-time; ChIP, chromatin Immunoprecipitation; HIF, hypoxia-inducible factor; ncRNA, noncoding RNA; kb, kilobase(s); TSS, transcription start site; HRE, hypoxia response element; PTM, post-translational modification.

In its latent (ligand unbound) state, AhR is found predominantly in the cytoplasm of the cell, and it is associated with the dimeric molecular chaperone heat shock protein 90 (Hsp90) and cochaperones (Kazlauskas et al., 1999). Ligand binding induces a conformational change of the receptor, resulting in its rapid nuclear translocation. In the nucleus, AhR dimerizes with aryl hydrocarbon receptor nuclear translocator (Arnt). The ligand-charged AhR/Arnt complex then binds to xenobiotic response elements (XREs) in regulatory regions of target genes and initiates transcription (Furness and Whelan, 2009; for review, see Denison et al., 2011). This process leads to rapid induction of phase I and phase II xenobiotic-metabolizing enzymes, which function to metabolize the activating ligands and thus provide negative feedback to dampen the AhR signaling. Persistent AhR signaling, such as that elicited by the unmetabolized ligand 2,3,7,8-tetrachlorodibenzo-*p*-dioxin (TCDD), is known to induce a broad spectrum of toxicological endpoints including thymic involution, teratogenicity, hepatotoxicity, tumor promotion, and wasting syndrome (Bock and Köhle, 2006).

In addition to its role in xenobiotic metabolism, studies also suggest roles for AhR in development. AhR-null mice show a range of phenotypic defects, including poor vascularization, impaired liver function, fibrosis, and decreased fertility (for review, see McMillan and Bradfield, 2007b), arguing for developmental and normal physiological functions of AhR. This finding is further supported by studies of invertebrate homologs of the AhR, which do not bind to any of the known AhR ligands. Instead, they regulate specific aspects of embryonic development (McMillan and Bradfield, 2007b). Furthermore, recent studies have also indicated roles for AhR in subsets of T cells, intraepithelial lymphocytes, and intestinal lymphoid follicles (Stevens et al., 2009; Kiss et al., 2011; Li et al., 2011).

The molecular mechanism for physiological AhR activation, independent of xenobiotics, is unknown. It has been reported that AhR can be activated by putative endogenous ligands, such as heme metabolites, lipoxin A4, prostaglandin G_2, and indirubin (Denison and Nagy, 2003). However, most of these endogenous ligands exhibit low binding affinity and are likely to be rapidly metabolized under normal physiological conditions. In addition, exposing cells to hydrodynamic shear stress or shear-conditioned serum (McMillan and Bradfield, 2007a), as well as switching cells from adherent to suspension culture or disrupting cell-cell contacts (Sadek and Allen-Hoffmann, 1994; Ikuta et al., 2004) have all been shown to activate the AhR. These alternative routes of AhR activation provide further experimental models for investigating the developmental and physiological functions of AhR.

A number of studies have attempted to separate physiologically activated AhR response genes from xenobiotic battery genes by comparing the gene expression profiles of TCDD and endogenous ligand-induced AhR activation (Adachi et al., 2004; de Waard et al., 2008; Henry et al., 2010). Despite the different experimental designs and different endogenous ligands being studied, the conclusions from these studies were very similar. It appeared that under each set of experimental conditions described, the gene expression profiles for both xenobiotic and endogenous ligands were essentially the same. However, cross-comparisons between these studies reveal distinct sets of target genes with little overlap among them. Thus, the spectrum of AhR target genes also seems to be cell context (e.g., cell type and developmental stage)-dependent.

To further characterize the physiological function of AhR, we decided to take an alternative approach by comparing the gene expression profiles of xenobiotic (YH439)-induced AhR activation with endogenous AhR activation, the latter being induced by switching adherent cell cultures to suspension cultures. We provide evidence that gene activation through AhR by both xenobiotics and suspension cultures is achieved via the same mechanism, mediated by recruitment of AhR to common XRE sites. However, the transcriptional output driven by AhR activation may differ, depending on the routes of activation, with suspension-activated AhR often leading to much broader, but more transient, changes in gene expression.

Materials and Methods

Plasmid Constructs. The pLV501 lentiviral expression vector was derived from pLV410G (gift from A/Professor Simon Barry, Women's and Children's Health Research Institute) digested with ClaI and EcoRV, replacing the gateway cassette with that of pLenti4/V5-DEST (Invitrogen, Carlsbad, CA) excised with ClaI and PmlI. To generate the pLV501_HisMyc_mAhR construct, His-Myc epitope-tagged full-length mouse AhR cDNA was recombined from the pENTR1A_ HisMyc_mAhR donor vector (Whelan et al., 2010) into the pLV501 destination vector by standard Gateway cloning (Invitrogen).

The control luciferase reporter plasmid pML-luc was made by removing CME enhancer elements from pML-6c-wt (gift from Professor J. Pelletier, McGill University) with BglII/EaeI digestion. To construct the pML-mTiparp-XRE reporter plasmid, a DNA fragment corresponding to 171 bp of the *Tiparp* intronic XRE enhancer was PCR-amplified from mouse genomic DNA with primers (5′ TTGGATCCACTCCACTCCTCTGCTTCC 3′ and 5′ TTGGATCCCCTCCTATCACACCAATC 3′) and inserted into the BamHI site of pML-luc.

Cell Cultures and Production of Stable Cell Lines. Mouse hepatoma Hepa-1c1c7 cells and AhR-null hepatocytes [*AhR*(−/−) Hepa] (Murray et al., 2005) were routinely grown in GIBCO minimum essential medium alpha, supplemented with 10% fetal calf serum, 100 U/ml penicillin, and 100 μg/ml streptomycin, and cultured at 37 and 34°C, respectively, with 5% CO_2. Dexamethasone was added to the hepatocyte culture medium at a 100 nM final concentration to promote cell survival. Stable polyclonal pooled mAhR reconstituted hepatocytes were generated by sequential infection of *AhR*(−/−) hepatocytes with lentivirus carrying the TetR expression plasmid (pLenti6/TR, blasticidin-resistant; Invitrogen) and HisMyc epitope-tagged mAhR expression plasmid [pLV501_HisMyc_mAhR, phleomycin (Zeocin)-resistant] and selected with either blasticidin (2.5 μg/ml) alone or in combination with phleomycin (100 μg/ml). Ectopic expression of the AhR is driven by the tetracycline-inducible promoter and can be increased by doxycycline treatment. However, because the background expression level of AhR in the reconstituted cells was indistinguishable from that of natural AhR expression levels in mouse hepatoma Hepa-1c1c7 cells (Fig. 1A), all experiments were conducted in the absence of doxycycline. The detailed protocols for lentivirus production and infection were described previously (Hao et al., 2011).

Human embryonic kidney (HEK) 293T cells and keratinocytes (HaCaTs) were routinely grown in GIBCO Dulbecco's modified Eagle's medium supplemented with 10% fetal calf serum, 2 mM L-glutamine, 100 U/ml penicillin, and 100 μg/ml streptomycin. Stable doxycycline-inducible AhR knockdown (HaCaT 4.2) or scramble shRNA control (HaCaT scramble) cells were generated by lentivirus-mediated infection as described previously (Hao et al., 2011) and were selected by fluorescence-activated cell sorting. For both stable cell lines, the overall green fluorescent protein-positive cells (i.e.,

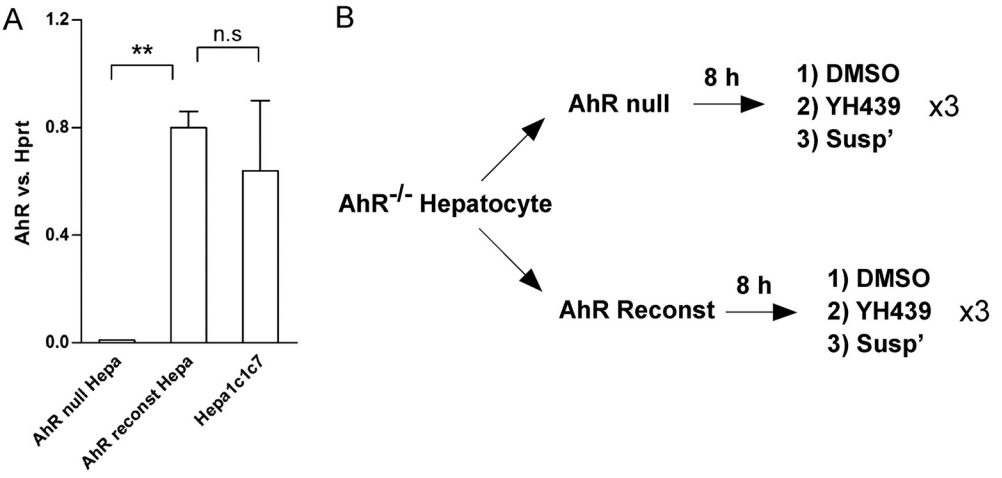

Fig. 1. Microarray design setup for the identification of specific AhR target genes in xenobiotic-treated and suspension-activated cells. A, qRT-PCR results showing the expression levels of *AhR* quantified in Hepa-1c1c7 cells and compared against immortalized AhR-null hepatocytes infected with control lentivirus (AhR-null Hepa) or lentivirus carrying HisMyc epitope-tagged AhR (AhR reconst Hepa). Data represent the mean ± S.E.M.; $n = 3$. **, $p < 0.01$; ns, not statistically significant. B, experimental setup of microarray experiments performed in mouse AhR-null and AhR reconstituted hepatocytes after 8 h of DMSO (0.1%), YH439 (10 μM) or suspension (Susp′) treatments. Three biological replicates were obtained for each cell line and treatment combination.

shRNA-expressing cells) after fluorescence-activated cell sorting were greater than 95%. Target sequences for AhR and scramble shRNA were 5′ CGTTTACCTTCAAAC 3′ and 5′ ACTACCGTTGTTATAGGTG 3′, respectively.

Suspension Cultures. Suspension cultures were prepared by dislodging cells from tissue culture flasks with 0.05% trypsin-530 μM EDTA, resuspension in semisolid media containing 1.68% methylcellulose, and incubation in the same manner as that for adherent cultures (Monk et al., 2001).

Microarray. Confluent mouse AhR-null hepatocytes stably expressing either TetR alone or in combination with HisMyc epitope-tagged mAhR were treated with vehicle alone (0.1% DMSO) or 10 μM YH439 or grown as suspension cultures for 8 h in biological triplicates. Total RNA was extracted using the RNeasy kit (QIAGEN, Valencia, CA) and profiled on the Bioanalyzer (Agilent Technologies, Santa Clara, CA) for RNA degradation. Then 500 ng of total RNA from each sample was reverse-transcribed into cDNA and in vitro-transcribed into biotin-labeled cRNA using the Illumina TotalPrep RNA Amplification Kit (Ambion, Austin, TX), and 1.5 μg of cRNA was hybridized to MouseWG-6 v2.0 Expression BeadChip (Illumina) microarrays according to the manufacturer's specification and scanned on the BeadArray Reader (Illumina) at scan factor 1. Microarray raw intensity values were background-subtracted using BeadStudio Data Analysis Software (Illumina) and normalized using the cross-correlation method (Chua et al., 2006). Differentially expressed transcripts for each condition were identified on the basis of a mean $\log_2$ fold change of at least 1.5-fold with a homoscedastic two-tailed t test $p < 0.05$ compared with the DMSO control for each cell line. Clustering was performed and generated using absolute correlation (centered) with centroid linkage on Cluster and TreeView (Eisen et al., 1998). Venn diagrams were generated using VENNY (an interactive tool for comparing lists with Venn diagrams; J. C. Oliveros, 2007; http://bioinfogp.cnb.csic.es/tools/venny/index.html). The raw and normalized microarray data were deposited into National Center for Biotechnology Information Gene Expression Omnibus with accession number GSE37144.

Transient Transfections and Dual Luciferase Assays. Triplicate wells were seeded with HEK 293T cells at 1.8×10^5 cells/well in a 24-well plate and grown for 16 h. Cells were transiently cotransfected with 200 ng of pML-luc or pML-mTiparp-XRE reporter plasmids, 0.1 ng of phRL-CMV *Renilla reniformis* luciferase plasmid (Promega, Madison, WI), 50 ng of Arnt expression plasmid (puro6_hArnt1), and 50 ng of AhR or Sim1 expression plasmids (puro6_AhR or puro6_Sim1) or empty control plasmid (puro6) using the FuGENE6 (Roche Diagnostics, Indianapolis, IN) transfection protocol. Cells were then treated with vehicle (0.1% DMSO) or YH439 (10 μM) 8 h after transfection and incubated for a further 16 h. For hypoxia experiments, cells were transiently cotransfected with 200 ng of pML-luc or pML-mTiparp-XRE reporter plasmids and 0.1 ng of phRL-CMV *R. reniformis* luciferase plasmid without Arnt or AhR overexpression plasmids. Eight hours after transfection, cells were either treated with hypoxia mimetic 2′2-dipyridyl (100 μM) or placed in a sealed container with a hypoxia sachet (Oxoid; Thermo Fisher Scientific, Waltham, MA) (<1% O_2) for 16 h. Relative luciferase units were calculated by measuring the firefly and *R. reniformis* luciferase activities using the GloMax Luminometer (Promega) as per the manufacturer's instructions.

Immunoblotting. Whole-cell extracts were prepared by lysing cells in a volume 3 times that of the cell pellet with WCE buffer (20 mM HEPES, pH 8.0, 420 mM NaCl, 0.5% IGEPAL CA-630, 25% glycerol, 0.2 mM EDTA, 1.5 mM $MgCl_2$, 1 mM dithiothreitol, and 1× protease inhibitors; Sigma-Aldrich, St. Louis, MO). Then 50 μg of cell lysate was separated on 10% acrylamide SDS-polyacrylamide electrophoresis gels and transferred onto nitrocellulose membranes by wet transfer (Bio-Rad Laboratories, Hercules, CA). Proteins were detected with monoclonal antibodies raised against AhR (RPT1; Abcam, Cambridge, MA) or α-tubulin (Serotec, Oxford, UK), and horseradish peroxidase-conjugated secondary antibodies, and visualized with Immobilon Western chemiluminescent substrate (Millipore Corporation, Billerica, MA).

RNA Extraction, cDNA Synthesis, and Quantitative Real-Time PCR. HaCaT 4.2 cells were cultured in the presence or absence of 1 μg/ml doxycycline for two continuous passages with medium change every 2 days. Confluent HaCaT 4.2 cells were treated with vehicle alone (0.1% DMSO) or 10 μM YH439 or grown in suspension cultures for 5 h. Total RNA was extracted, of which 2 μg was reverse transcribed to cDNA as described previously (Hao et al., 2011). RNA was also extracted from hypoxia-treated Hepa-1c1c7 cells or Hepa-1c1c7 cells stimulated with vehicle alone (0.1% DMSO), 10 μM YH439, or 10 nM TCDD or grown in suspension cultures for 2, 5, and 8 h and reverse transcribed into cDNA. All hypoxia treatment was performed in a Ruskinn Invivo$_2$ 400 hypoxia workstation (Oxoid;, Thermo Fisher Scientific) set to 1% O_2 and 5% CO_2.

Intron-spanning quantitative real-time (qRT)-PCR primers were designed using Primer3Plus (http://www.bioinformatics.nl/cgi-bin/primer3plus/primer3plus.cgi). The primer sequences as well as primer efficiencies and amplicon sizes are listed in Supplemental Table 4. Target gene expression was normalized against housekeeping genes hypoxanthine-guanine phosphoribosyltransferase (*Hprt*) and polymerase (RNA) II (DNA directed) polypeptide A (*POLR2A*), for mouse and human samples, respectively. All experiments were performed in technical triplicates for three biological replicates.

Chromatin Immunoprecipitation. Hepa-1c1c7 cells were seeded on 75-cm^2 tissue culture flasks and grown to confluence. Cells were treated with vehicle alone (0.1% DMSO) or 10 μM YH439 or grown in suspension cultures for 5 h. Hypoxic cells (1% O_2) were also prepared by transferring cells to a Ruskinn Invivo$_2$ 400 hypoxia chamber and incubated for 4 h. Chromatin immunoprecipitation

(ChIP) was performed with antibodies against either AhR (RPT9; Abcam), hypoxia-inducible factor (HIF)-1α (Abcam), Myc epitope tag (Abcam), or nonspecific control IgG (Millipore/Jackson ImmunoResearch Laboratories, West Grove, PA) as described previously (Farrall and Whitelaw, 2009). Fold enrichment was calculated using the $2^{-\Delta\Delta Ct}$ method, where ΔΔCt represents the difference between threshold cycles of experimental antibodies over the type-matched IgG control. All real-time PCR quantification of ChIP enrichments was performed in technical triplicates for three biological replicates. Primer sequences used in the ChIP experiments are listed in Supplemental Table 5.

Electrophoretic Mobility Shift Assay. Hepa-1c1c7 cells were treated with vehicle alone (0.1% DMSO) or 10 μM β-naphthoflavone or grown in suspension cultures for the durations indicated in Supplemental Fig. 3. Nuclear extracts were collected, and 8 μg was assayed by electrophoretic mobility shift assay for ^{32}P-labeled XRE binding as described previously (Hao et al., 2011).

Bioinformatics. Genome-wide distribution of XRE oligomers (G[CGTG]$_n$ or [GCGTG]$_n$) was identified from the mouse reference genome (NCBI37/mm9 assembly) using the Genomic Short-read Nucleotide Alignment Program (GSNAP) program (Wu and Nacu, 2010). Neighboring XRE concatemers (<100 bp apart) stemming from a single long XRE concatemer were only counted once. Distribution maps were generated with Cis-regulatory Element Annotation System (CEAS) tools available from http://liulab.dfci.harvard.edu/CEAS/index.html.

Statistical Analysis. Quantitative data are expressed as means ± S.E.M. from at least three independent experiments unless otherwise specified. Significant differences were evaluated using an unpaired Student's *t* test (two tails for gene expression analysis and one tail for fold enrichment). The levels of significance are as follows: *, $p < 0.05$; **, $p < 0.01$; and ***, $p < 0.001$.

Results

Microarray Analyses Reveal Differential Gene Regulation between Ligand- and Suspension-Activated AhR in Mouse Hepatocytes. To determine the differences between AhR-dependent gene regulation in response to exogenous ligands or endogenous activation of AhR invoked by switching cells from adherent to suspension culture, genome-wide microarray expression studies were conducted. We compared the gene expression profiles in mouse AhR-null hepatocytes, obtained via immortalization of hepatocytes from an AhR-null mouse (Murray et al., 2005), and immortalized null hepatocytes reconstituted to stably express the mouse AhR. The expression levels of AhR in the reconstituted cells are indistinguishable from AhR expression levels in mouse hepatoma Hepa-1c1c7 cells (Fig. 1A).

Our microarray design incorporated a total of six conditions (Fig. 1B), with three biological replicates for each cell type and treatment. To identify differentially expressed genes that are reproducibly regulated across all biological replicates for each condition by at least 1.5-fold over the DMSO control for each cell line, a Student's *t* test was performed at a threshold $p < 0.05$ to filter out probe sets with high variability. With use of this statistical analysis, all samples can be correctly clustered according to conditions and cell types (Fig. 2A), suggesting that specific transcriptional differences can be distinguished. Thus, differential expression was likely to be driven by differences in cell types and treatments instead of technical variation between biological replicates.

As shown in the four-set Venn diagram (Fig. 2B), only a small number of transcripts (<50) responded to YH439 in AhR-null hepatocytes by >1.5-fold. This result is consistent with another study showing that the ligand-induced changes in gene expression are entirely AhR-dependent (Tijet et al., 2006). In contrast, significantly more (i.e., 112) transcripts were regulated in YH439-treated AhR reconstituted cells (Fig. 2, B and C). However, switching cells from adherent to suspension cultures appeared to be a stronger driving force for inducing differential gene expression, which altered the abundance of more than 3000 transcripts. Approximately half of these suspension-regulated genes seen in AhR reconstituted hepatocytes were AhR-independent (also differentially expressed in the AhR-null hepatocytes). However, there were 1463 transcripts whose expression was altered specifically in the presence of AhR, suggesting that the breadth of endogenously activated AhR targets was much wider than that of xenobiotic-regulated genes.

According to our microarray results, the AhR target genes can be broadly divided into three classes: I, regulated predominantly by xenobiotics; II, regulated predominantly by suspension culture; and III, regulated by both xenobiotics and suspension culture (Fig. 2B). Of interest, most of the classic xenobiotic-metabolizing AhR target genes, including *Cyp1b1* (cytochrome P450 1b1), *Nqo1* [NAD(P)H quinone oxidoreductase 1], and *Aldh3a1* (aldehyde dehydrogenase 3a1) belong to class III (Table 1). One of the hallmark events of AhR activation is the induction of *Cyp1a1* gene expression. This target gene was not isolated in the microarray analysis because there was no hybridization signal due to probe failure. However, subsequent quantitative qRT-PCR experiments confirmed the induction of *Cyp1a1* genes in both ligand- and suspension-treated AhR reconstituted hepatocytes (Supplemental Fig. 1). We therefore confirm and classify *Cyp1a1* as a bona fide class III AhR target gene.

Statistical analysis of the microarray data suggested that AhR could function as both a transcription activator and transcription repressor. Under acute conditions (8 h), the predominant effect of AhR was up-regulation of gene expression. However, in the longer term assessed by comparing steady-state nontreated AhR-null cells against AhR reconstituted cells, significantly more genes were down-regulated in the AhR reconstituted cells (Fig. 2C, last bar), implying a chronic repressive function for AhR. Consistent with our results, AhR-mediated long-term repression has also been reported by others when liver tissues from AhR(+/+) and *AhR*(−/−) mice were compared (Tijet et al., 2006). How this long-term repression is achieved is not known, although epigenetic mechanisms, induction of transcription repressor genes or noncoding RNA (ncRNA), and transcription factor cross-talk are possible candidates. In terms of the latter, ligand-activated AhR has been reported to inhibit both cell cycle progression and acute-phase inflammatory gene expressions in hepatocytes by forming repressive complexes with Rb (retinoblastoma) and E2F or modulating nuclear factor-κB signaling pathways (Marlowe et al., 2004; Patel et al., 2009).

Validation of Microarray Result by qRT-PCR. To validate the microarray results, selected AhR target genes from each class were analyzed by qRT-PCR in both immortalized hepatocytes and in an independent and classically used hepatoma cell line for AhR signaling, Hepa-1c1c7 (Table 1; Fig. 3). Because AhR is known to bind to the *Cyp1a1* and *Cyp1b1* gene promoters in an oscillatory manner (Hestermann and

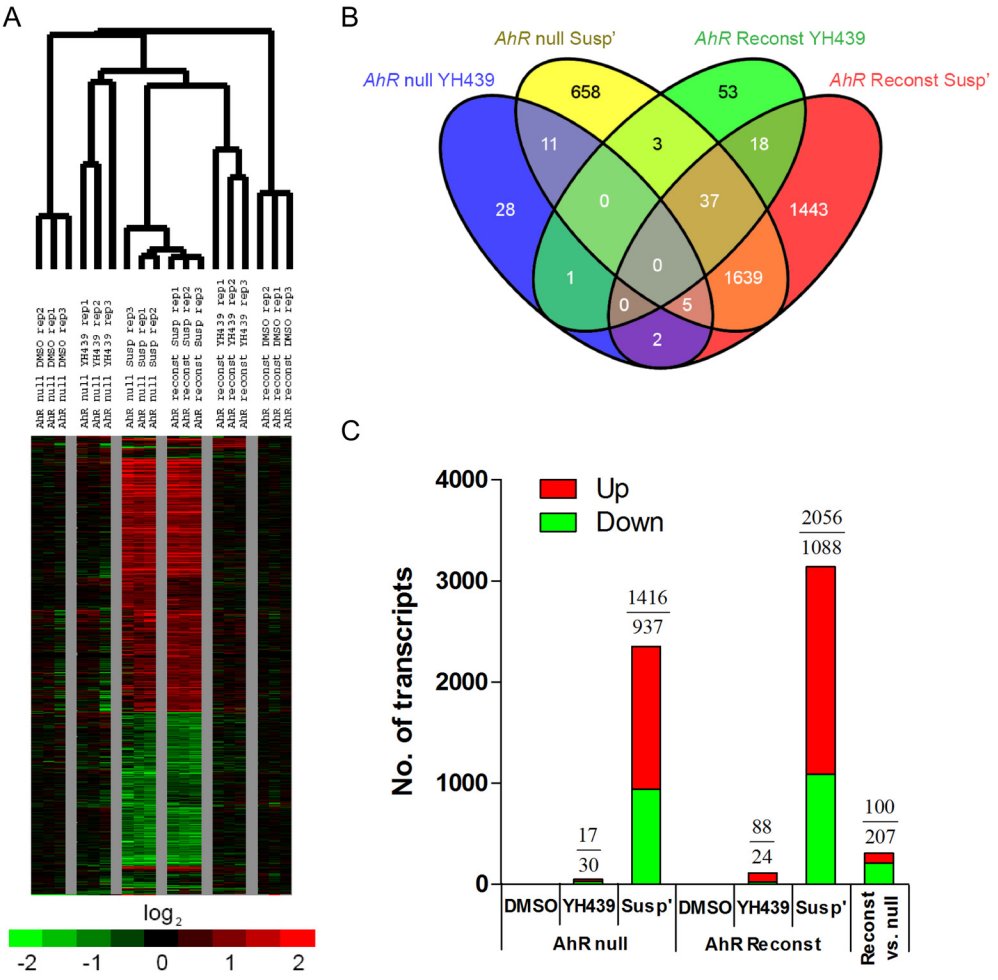

Fig. 2. Microarray analysis identifies distinct transcriptional responses between ligand- and suspension-activated AhR. A, heatmap and hierarchical clustering analysis of probes with more than 1.5-fold changes in their expression. Data represent $\log_2$ fold change for each cell line and condition compared with that for the DMSO control after filtering with Student's *t* test for probes with $p < 0.05$. Red, up-regulated by 1.5-fold and greater; green, down-regulated by 1.5-fold or greater. B, four-set Venn diagram showing all transcripts with more than 1.5-fold expression changes, according to the indicated cell lines and treatments. Number of genes in class I, II, and III AhR target genes are 53, 1443, and 18, respectively. C, number of transcripts up- or down-regulated (>1.5-fold) in each cell line/treatment compared with that for the DMSO control of each cell line. Reconst, reconstituted; Susp′, suspension.

Brown, 2003), RNA samples were extracted at different time points to capture the temporal expression pattern of these target genes after AhR activation. In general, the qRT-PCR results agreed well with the microarray data for most of the AhR-inducible genes. One exception is *Spint1*, a Kunitz type 1 serine protease inhibitor that showed induction by ligand

TABLE 1

Summary of microarray and qRT-PCR results for selected AhR target genes

Numbers indicate fold changes over DMSO control; values >1 represent up-regulated genes, whereas values <1 represent down-regulated genes; — indicates no change. Statistically significant fold changes are in bold.

	Microarray (Hepatocyte), 1.5-Fold Cutoff ($p < 0.05$)					qRT-PCR (Hepatoma Hepa-1c1c7)								
	Null		Reconst		Reconst/Null DMSO	YH439			TCDD			Susp		
	YH439	Susp	YH439	Susp		2 h	5 h	8 h	2 h	5 h	8 h	2 h	5 h	8 h
Class I														
Por	—	—	**2.1**	—	1.0	**1.3**	**1.6**	**1.9**	**1.2**	1.4	**1.6**	—	—	—
Cldnd1	—	—	**2.1**	—	0.9	**1.5**	**2.1**	**1.9**	**1.4**	**2.0**	**2.1**	—	—	—
Mical2	—	—	**0.7**	—	1.1	—	0.8	0.8	0.8	**0.7**	—	—	**1.7**	1.3
Class II														
ApoER2 (Lrp8)	—	—	—	**2.0**	1.2	**0.5**	**0.5**	—	**0.5**	**0.4**	—	**0.5**	—	**1.5**
Ganc	—	—	—	**0.6**	1.1	**0.3**	—	**1.3**	**0.3**	—	**1.4**	**0.2**	**0.5**	**0.7**
Class III		—	—											
Cyp1a1[a]	—	**2.5**	**16.2**	**9.2**	7.6	**6.2**	**15.0**	**17.9**	**7.0**	**13.4**	**19.6**	**3.5**	**9.8**	**6.3**
Cyp1b1	—	**0.5**	**3.3**	**2.1**	1.4	**7.5**	**15.4**	**12.0**	**7.1**	**15.9**	**15.2**	**3.0**	**12.3**	**10.7**
Nqo1	—	—	**2.2**	**2.0**	1.9		**4.3**	**9.1**		**4.2**	**6.7**	0.7	**2.0**	**3.0**
GTRAP3-18 (Arl6ip5)	—	—	**1.6**	**1.6**	1.3	**2.0**	**3.0**	**2.3**	**2.1**	**3.4**	**2.4**	**1.3**	**1.8**	**1.4**
Spint1 (HAI-1)[b]	—	—	**1.9**	**1.9**	1.1	5.4	4.6	**3.5**	6.2	**6.3**	**5.0**	—	—	—
Serpinb2 (Pai2)	—	**0.6**	**2.1**	**2.0**	0.5	**1.7**	**2.2**	1.6	1.8	**2.1**	1.7	1.6	1.6	—
Tiparp	—	**2.4**	**3.6**	**3.6**	0.9	**14.4**	**9.6**	**7.4**	**18.9**	**9.0**	**9.6**	**9.3**	**3.2**	**2.1**
4931440P22Rik	N.A.	N.A.	N.A.	N.A.	N.A.	**2.3**	**2.3**	**2.7**	**3.6**	**2.4**	**2.9**	**2.2**	**1.4**	**1.5**

Reconst, reconstituted; Susp, suspension; N.A., probes not available on the microarray chips.

[a] Expression determined by qRT-PCR (Supplemental Fig. 1).

[b] The *Spint1* gene is one of the rare incidences that showed differential gene regulation between hepatocytes and hepatoma cells, making it a class III AhR target gene in immortalized hepatocytes but a Class I AhR target in hepatoma cells.

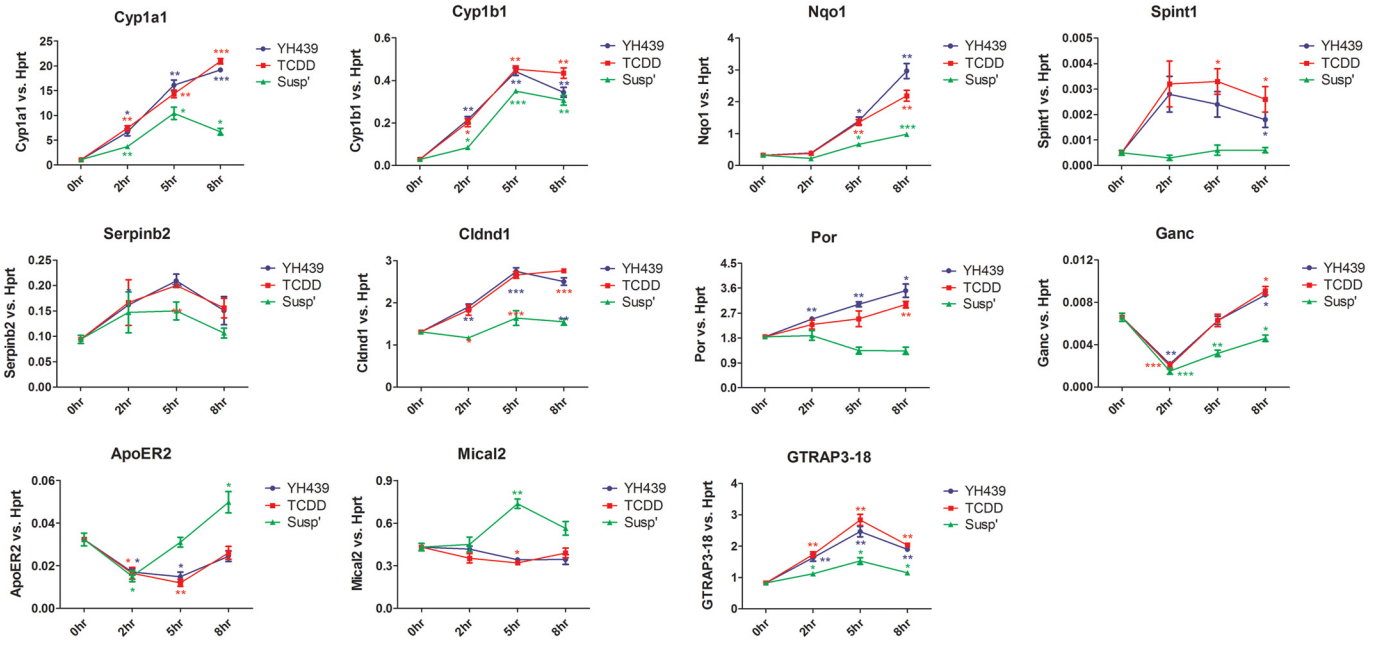

Fig. 3. qRT-PCR validation of xenobiotic and suspension regulated AhR target genes. Temporal expression pattern of genes in confluent Hepa-1c1c7 cells treated with YH439 (10 μM) or TCDD (10 nM) or grown in suspension cultures (Susp′) for the time indicated. Gene expression levels were measured by qRT-PCR after normalization against the *Hprt* reference gene. Data represent the mean ± S.E.M.; $n = 3$. Significant differences were determined using an unpaired Student's t test: *, $p < 0.05$; **, $p < 0.01$; ***, $p < 0.001$.

and suspension culture in AhR reconstituted hepatocytes (Supplemental Fig. 2) but was up-regulated only by ligand treatments in Hepa-1c1c7 cells (Table 1; Fig. 3). This discrepancy could result from intrinsic differences between cell lines, because our microarray experiment was performed in immortalized mouse hepatocytes, whereas the subsequent validation was performed in hepatoma cells. Similar cell line to cell line variations have been widely reported from other AhR microarray studies (Kim et al., 2009). However, the fact that the vast majority of AhR target genes tested responded in the same way between the two cell lines suggested that the changes in gene expression were likely to reflect genuine trends in AhR-mediated gene expression.

Our analysis also revealed genes that were subjected to repression by either ligand- or suspension-activated AhR (Table 1; Fig. 3). Both the *Ganc* (neutral α-glucosidase C) and *ApoER2* (apolipoprotein E receptor 2) genes were repressed in the short term (2–5 h) but returned to baseline or slightly elevated expression after 8 h of treatment. The short-term response implies a novel, active repression by the AhR that may be relieved via protein turnover of the activated AhR, which has previously been shown to be mostly degraded after 8 h of ligand or suspension treatments (Cho et al., 2004) (Supplemental Fig. 3). Our time course quantification of AhR-induced gene expression also showed some genes (*Serpinb2*, *Spint1*, and *GTRAP3-18*) to be activated transiently before declining back toward baseline levels (Table 1; Fig. 3). Alternatively, genes encoding for xenobiotic-metabolizing proteins such as *Cyp1a1, Cyp1b1*, *Nqo1*, and *Por* (P450 (cytochrome) oxidoreductase) maintained increased levels of expression or continued to augment across all time points, which is consistent with a previous report showing sustained *Cyp1a1* and *Nqo1* expression in TCDD-treated Hepa-1c1c7 cells or hepatic tissue of C57BL/6 mice (Dere et al., 2006).

The effect of YH439-elicited AhR activation was also compared with that elicited by the prototypical AhR ligand TCDD. A previous study by our laboratory suggested that YH439 has a novel mode of activation, which does not require full access to the AhR ligand-binding pocket (Whelan et al., 2010). As a result, the possibility that YH439 may regulate some AhR target genes differentially from TCDD exists. However, for all the genes tested, there was very little difference between the two ligands, either directionally or in terms of the magnitude of gene expression (Fig. 3).

Xenobiotics and Switching Cells from Adherent to Suspension Cultures Activate AhR Target Genes via the Same XRE Sites. Both xenobiotics (YH439 and TCDD) and switching cells from adherent to suspension cultures activate AhR and induce AhR target gene expression (Table 1). It is well accepted that the xenobiotic-dependent AhR transcriptional response is mediated through recruitment of the AhR at target XRE sites. We confirmed this finding and showed that AhR was recruited to the *Cyp1a1* and *Cyp1b1* promoters during receptor activation by the atypical AhR ligand YH439 (Fig. 4). In addition, we showed that switching cells from adherent culture to suspension also led to AhR recruitment at the same XRE enhancer elements, although to a lesser extent, suggesting that these two different routes of AhR activation drive the same gene regulatory mechanism. The reduced AhR occupancy after suspension culturing was consistent with qRT-PCR results showing reduced *Cyp1a1* and *Cyp1b1* expression in response to suspension treatments compared with that to YH439 (Fig. 3).

AhR Coordinates *Tiparp* and Overlapping *4931440P22Rik* Antisense ncRNA Expression. From the microarray analysis, the *Tiparp* [TCDD-inducible poly(ADP-ribose) polymerase] gene was shown to be strongly inducible by YH439 in AhR reconstituted hepatocytes (Table 1). *Tiparp* is a recently described AhR target gene that is commonly up-regulated in cells exposed to TCDD and other AhR ligands

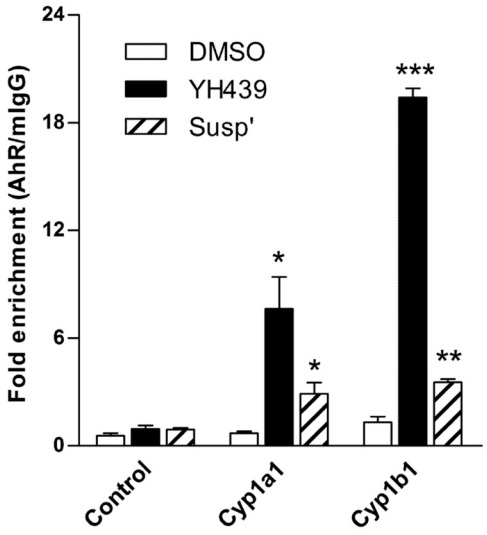

Fig. 4. AhR is recruited to *Cyp1a1* and *Cyp1b1* promoters after ligand- and suspension-dependent AhR activation in Hepa-1c1c7 cells. Fold enrichment of DNA fragments bound by AhR after 5 h of YH439 (10 μM) or suspension (Susp′) treatments, expressed as a ratio over the type match control IgG antibody ChIP. The control primer set was designed to target an intronic region of mouse *Spint1* gene, which does not contain any XRE consensus sequence. Data represent the mean ± S.E.M.; $n = 3$. Significant differences were calculated using an unpaired Student's t test: *, $p < 0.05$; **, $p < 0.01$; ***, $p < 0.001$.

(Dere et al., 2006; Tijet et al., 2006; Henry et al., 2010). Although the cellular function of this gene is currently unknown, a recent study suggests that TCDD-dependent *Tiparp* induction could be a factor linking TCDD exposure and wasting syndrome, because induction of *Tiparp* by TCDD reduces cellular levels of NAD^+ and decreases hepatic gluconeogenesis (Diani-Moore et al., 2010). In addition to ligand treatments, switching adherent cells to suspension cultures also up-regulated *Tiparp*, which was seen in both AhR-null and AhR reconstituted hepatocytes (Table 1). However, the fold induction of *Tiparp* expression is larger in reconstituted hepatocytes than in null cells (3.6-fold versus 2.4-fold), suggesting a role of AhR in suspension-induced *Tiparp* transcription. To further confirm the role of AhR in *Tiparp* expression, we used a doxycycline-inducible AhR knockdown human keratinocyte cell line. Despite the differences in species and cell types, knockdown of human *AHR* in HaCaT cells completely abrogated both ligand- and suspension-dependent human *TIPARP* gene induction, confirming that activation of AhR is a genuine mode of regulation for *Tiparp* expression (Fig. 5).

Inspection of the mouse *Tiparp* genetic locus also identified a ncRNA (*4931440P22Rik*, also known as *Tiparp-as1*), running in the opposite direction to the protein coding *Tiparp* gene (Fig. 6A). Because part of the *Tiparp-as1* transcript overlaps with the 5′ region of the *Tiparp* gene (Fig. 6A), we hypothesized that this ncRNA could be transcriptionally regulated by AhR in the same way as the protein coding *Tiparp* gene. This hypothesis was indeed supported by qRT-PCR analysis, in which the temporal expression pattern of *Tiparp-as1* mirrored that of *Tiparp* for both ligand- and suspension-treated cells across all three time points (Fig. 6B). This is the first experimentally validated example to link the AhR signaling pathway with noncoding RNA expression. Similar concordant expression in coding mRNA/ncRNA pairs has also

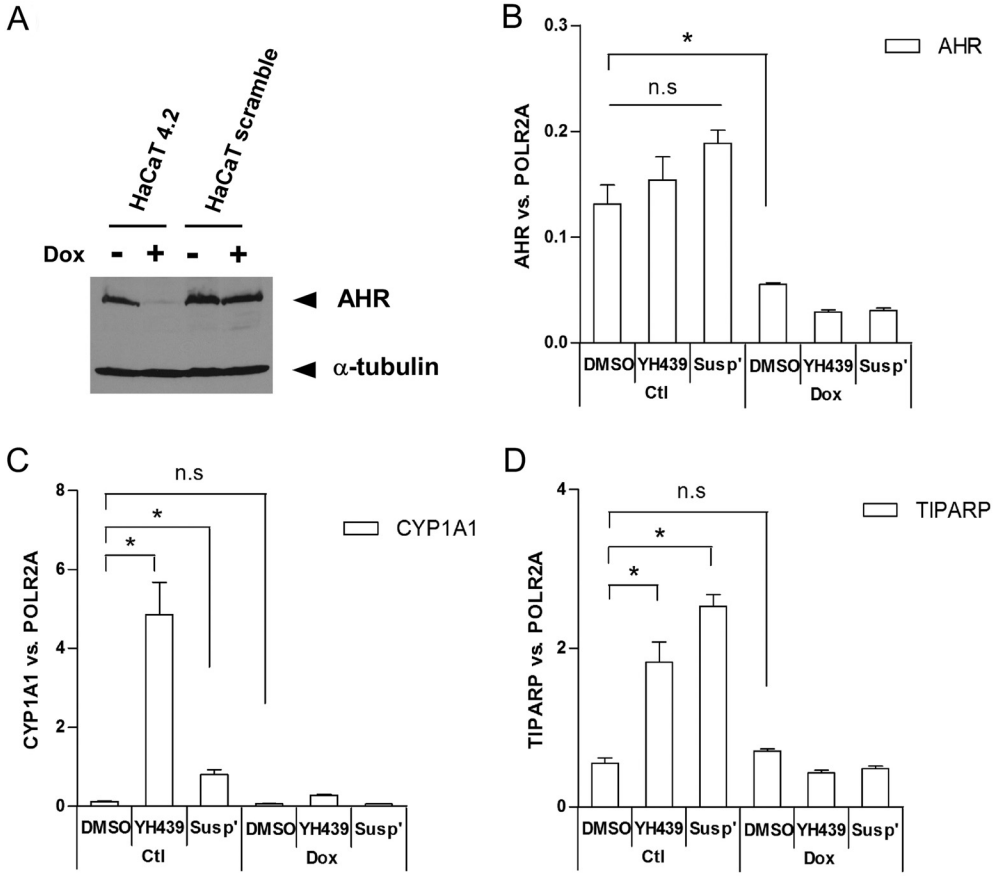

Fig. 5. Knockdown of *AHR* in HaCaT cells abolishes both ligand- and suspension-dependent AHR activation. qRT-PCR results of doxycycline-induced *AHR* knockdown repressing AHR expression at both (A) protein and (B) mRNA levels in human HaCaT cells. C and D, knockdown of *AHR* in HaCaT 4.2 cells greatly reduced *CYP1A1* induction and completely abolished *TIPARP* induction after 5-h YH439 (10 μM) treatments or culturing in suspension conditions (Susp′). Relative gene expression was normalized against the *POLR2A* housekeeping gene. Data show the mean ± S.E.M.; $n = 3$. *, $p < 0.05$; ns, not statistically significant.

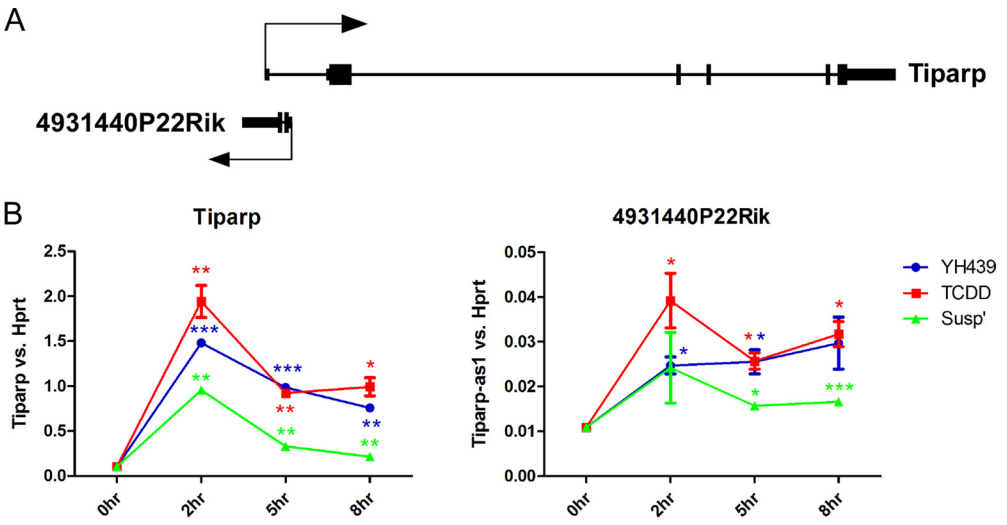

Fig. 6. AhR coordinates the expression of both *Tiparp* and the overlapping *4931440P22Rik* (*Tiparp-as1*) antisense ncRNA expression. A, genomic organization of the murine *Tiparp-4931440P22Rik* locus, the directions of transcription are indicated by arrows. B, relative expression profiles of *Tiparp* and *Tiparp-as1* measured by real-time qRT-PCR in Hepa-1c1c7 cells treated with YH439 (10 μM), TCDD (10 nM), or cultured in suspension conditions (Susp′) for 2, 5, and 8 h. Data denotes the mean ± S.E.M.; $n = 3$. Significant differences were identified using unpaired Student's t test: *, $p < 0.05$; **, $p < 0.01$; ***, $p < 0.001$.

been described for lineage commitment genes such as *Evx1/Evx1as* and *Hoxb5/Hoxb5as* during embryonic stem cell differentiation (Dinger et al., 2008), although the functions of these ncRNAs were not defined.

AhR-Dependent *Tiparp/Tiparp-as1* Induction Is Regulated by the Same XRE Enhancer Element. The mouse *Tiparp* gene spans an ~27-kb region on chromosome 3, encompassing 6 exons. There are a total of 24 XRE core elements (GCGTG) in the region from 10 kb upstream of the transcription start site (TSS) of *Tiparp* to the end of the transcribed region. Six of them are clustered together within a 45-bp fragment, including 4 tandem repeats of XRE core elements ($G[CGTG]_4$) arranged in a concatemer configuration (Fig. 7A). A similar XRE configuration has been identified at the promoter region of the AhR-inducible *Cyp2s1* gene (Rivera et al., 2007). Response element concatemerization may increase the avidity of enhancer/transcription factor interaction, which may be important in the context of gene activation from histone-bound DNA. Consistent with this notion, *Tiparp* is an immediate early target gene whose expression peaks as early as 2 h after AhR activation (Fig. 6).

The XRE cluster of the *Tiparp* gene is positioned in the first intron, ~1.2 kb downstream of the TSS and ~200 bp upstream of *Tiparp-as1* (Fig. 7A). Given the coordinated expression pattern of these transcripts, we hypothesized that both transcripts could be regulated by this concatemerized XRE. Our ChIP experiments, with two independent primer sets flanking the same XRE concatemer sequence, showed statistically significant enrichment of AhR binding after YH439 treatment (Fig. 7B). Similar enrichment was not detected when Hepa-1c1c7 cells were switched from adherent to suspension cultures, presumably because of reduced AhR complex binding (Supplemental Fig. 3) coupled with relative low binding affinity of the AhR antibody. For comparison, we therefore used AhR-null hepatocytes that constitutively express HisMyc epitope-tagged mouse AhR (Whelan et al., 2010). In agreement with our qRT-PCR data (Fig. 6), when tagged AhR was ChIPed using anti-Myc tag antibodies in the reconstituted hepatocytes, significant binding of AhR was captured at the XRE concatemer site of *Tiparp* in both YH439-treated and suspension cells (Fig. 7C).

To further test the role of the XRE concatemer in regulating AhR-mediated gene expression, a luciferase reporter construct driven by a 67-bp minimum adenovirus pML and a 171-bp XRE enhancer element cloned from *Tiparp* intron 1 was generated. Transient cotransfection of this reporter construct with the AhR expression plasmid in HEK 293T cells led to strong luciferase reporter induction even in the absence of AhR ligands (Fig. 7D). This effect was AhR-specific, because similar induction was not observed with overexpression of the related bHLH/PAS protein Sim1 (Fig. 7D).

In addition to being regulated by xenobiotics, the concatemer of overlapping XREs in the promoter of the *Cyp2s1* gene has also been shown to function as a hypoxia response element (HRE) recognized by the bHLH/PAS HIFs, thus contributing to the hypoxia inducibility of this gene (Rivera et al., 2007). Because the XRE concatemer sequence identified from the *Tiparp/Tiparp-as1* locus resembles that of *Cyp2s1*, we tested whether a similar mode of regulation could also apply to the *Tiparp/Tiparp-as1* genes. Reporter gene assays were performed in 293T cells transfected with either pML control plasmid or pML-mTiparp-XRE plasmid and treated with the HIF-activating hypoxia mimetic 2′2-dipyridyl or grown under hypoxia (<1% O_2) for 16 h. Consistent with what has been reported for the *Cyp2s1* gene, the 171-bp enhancer of the *Tiparp* gene was also sensitive to these treatments (Fig. 7D). Furthermore, exposure of Hepa-1c1c7 cells to hypoxia also led to HIF-1α recruitment at the XRE concatemer site of *Tiparp* (Fig. 7E) and induced *Tiparp* gene expression (Fig. 7F). Thus, our results provide the second example for which overlapping XRE enhancer elements may function as both XREs and HREs to regulate gene expression.

In addition to *Cyp2s1* and *Tiparp* loci, XRE concatemerization was also found at ~22 kb upstream of *Serpinb2* (also known as Pai2 or plasminogen activator inhibitor-2), another known target of AhR (Table 1; Fig. 3). We became interested in this XRE cluster site because no XRE core element was identified for *Serpinb2* within 10 kb of its TSS, even though the XRE core is expected to occur every 512 bp on average (40 times in a 20-kb DNA fragment). The lack of XRE sites in close proximity to the *Serpinb2* promoter is even more remarkable, given that previous genome-wide studies suggest that more than 99.98% of all mouse genes have at least one XRE core element within 10 kb of their TSS, regardless of whether they are AhR-responsive or not (Dere et al., 2011). We reasoned that although the identified XRE concatemer

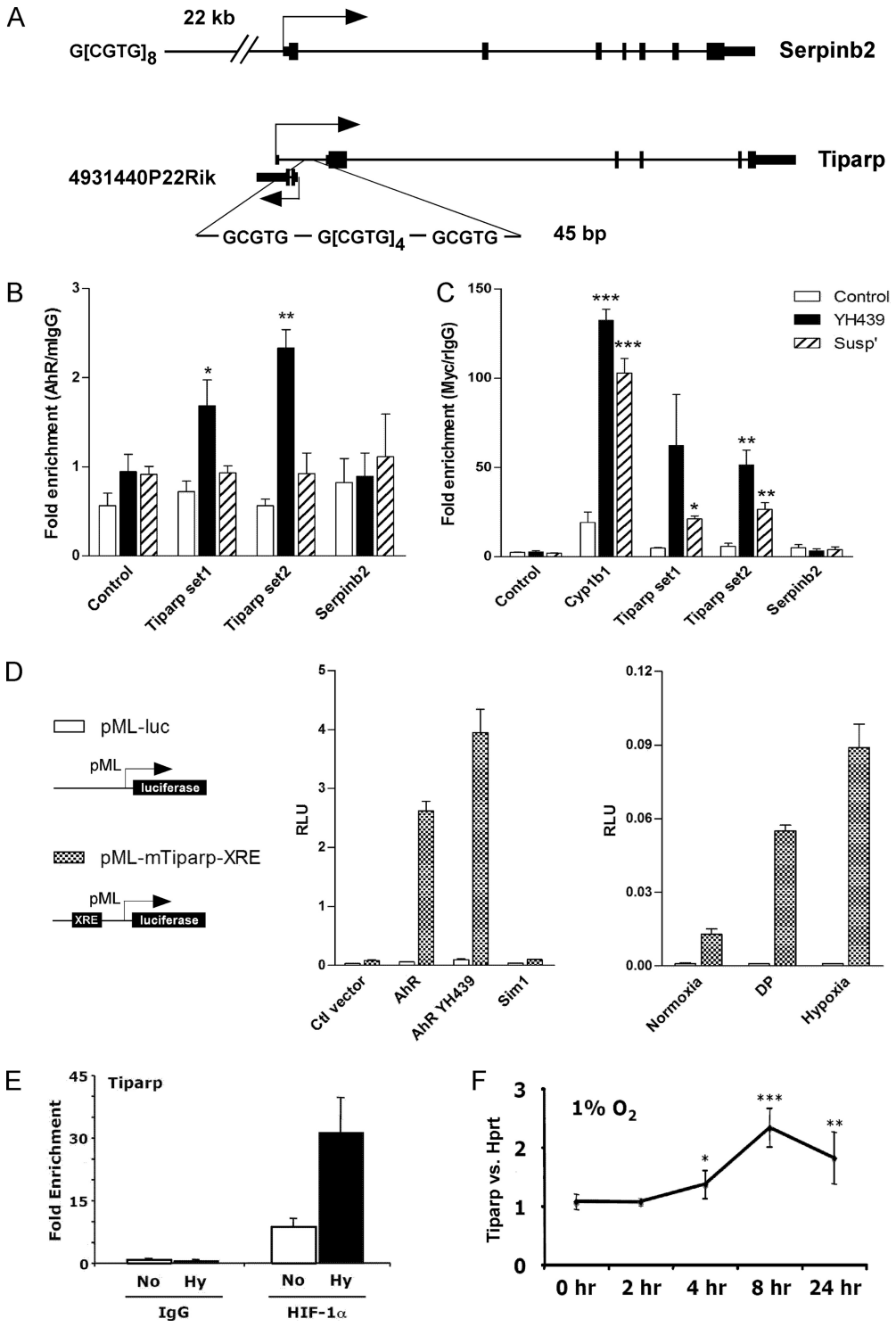

Fig. 7. The murine *Tiparp* XRE enhancer region is bound directly by AhR and regulated by xenobiotic ligand treatments. A, genomic organization of the murine *Tiparp* and *Serpinb2* loci, indicating the relative position of XRE concatemers. B and C, ChIP experiments showing YH439 (10 μM)-dependent binding of endogenous (B) and HisMyc epitope-tagged (C) AhR at the intronic XRE site of the *Tiparp* gene. Similar AhR recruitment was also observed when adherent cultures were switched to suspension in HisMyc epitope-tagged AhR reconstituted AhR-null hepatocytes. In contrast, no AhR enrichment was observed with non-XRE spanning *Spint1* control primers or primers designed to target the *Serpinb2* distal XRE concatemer site. Tiparp set1 and set2 represent two different sets of primers targeting overlapping regions of the *Tiparp* XRE concatemer. Data are mean ± S.E.M.; $n = 3$. *, $p < 0.05$; **, $p < 0.01$; ***, $p < 0.001$. D, left, schematic diagram of luciferase assay constructs; middle, activation of pML-mTiparp-XRE reporter construct in HEK 293T cells by transient transfection of AhR expressing plasmid both in the presence and in the absence of ligand (YH439, 10 μM), but not with overexpression of Sim1; right, activation of pML-mTiparp-XRE but not the control pML reporter constructs via 16 h of hypoxia (<1% O_2) or hypoxia mimetic 2′2-dipyridyl (100 μM) treatments. Data indicates mean ± S.D. of transfections performed in triplicate and are representative of three independent experiments. RLU, relative luciferase units; E, exposure of Hepa-1c1c7 cells to hypoxia (Hy) led to HIF-1α recruitment at XRE concatemer site of *Tiparp*. Data are the mean ± S.E.M.; $n = 3$. No, normoxia. F, induction of *Tiparp* gene expression during hypoxia (1% O_2). Data are the mean ± S.E.M.; $n = 3$. *, $p < 0.05$; **, $p < 0.01$; ***, $p < 0.001$.

site is positioned more than 20 kb upstream of *Serpinb2*, it may still function as an enhancer element of *Serpinb2* and regulate *Serpinb2* expression by DNA looping. To test this hypothesis, ChIP assays were performed with antibodies against either endogenous AhR in Hepa-1c1c7 cells or Myc tag antibodies against HisMyc epitope-tagged AhR in AhR reconstituted hepatocytes. However, unlike the XRE concatemer site at intron 1 of the *Tiparp* gene, no AhR enrichment was observed at the remote XRE site of the *Serpinb2* gene (Fig. 7, B and C). Thus, the existence of the XRE concatemer alone does not necessarily result in AhR recruitment, and AhR dependent up-regulation of *Serpinb2* transcription might be achieved via partnering of AhR with other transcription factors that recognize alternative motifs independent of XRE. Of note, AhR has been shown to be recruited to the XRE-like sequence (AhRE II) in some AhR-inducible genes (Boutros et al., 2004; Sogawa et al., 2004), and most recently a nonconventional, Arnt-independent XRE was defined (Huang and Elferink, 2012). Furthermore, in agreement with the above reports, genome-wide ChIP-on-chip

studies suggested that a large proportion of the AhR binding sequences did not harbor canonical XREs (Ahmed et al., 2009; Pansoy et al., 2010).

Of interest, genome-wide in silico analysis revealed thousands of XRE concatemer sites in the mouse genome (Supplemental Table 2). These XRE concatemers seem to be randomly distributed across all chromosomes except for the sex chromosomes (Supplemental Fig. 4). Similar genomic distribution has also been independently observed with the XRE core sequence (Dere et al., 2011). Of the 2665 XRE concatemer sites (defined as genome locations with four or more direct repeats of XRE cores), 78 of them fall within proximal promoter regions (±3 kb of TSS) of known genes (Supplemental Table 3). Apart from *Tiparp*, 30 of these genes were expressed at levels significantly high enough to be detected by microarray analysis. Of these, 9 showed altered expression upon suspension treatment, whereas none were altered by ligand stimulation. Of the nine suspension-altered genes, only four were altered in an AhR-dependent manner. Thus, cross-comparison between the microarray data and the XRE concatemer sites showed no apparent correlation between these two data sets. It was also noted that, in addition to the overlapping CGTG elements (i.e., G[CGTG]$_n$), we also identified at least seven incidences for which we saw GCGTG concatemerization ([GCGTG]$_n$, n >4), although none of these XRE concatemers were located in the proximal promoter regions of AhR target genes (Supplemental Table 2). Nevertheless, both of these XRE concatemer configurations give rise to (G/T)NGCGTG that matches well with the XRE consensus sequence (Lusska et al., 1993).

Discussion

The mechanism of xenobiotic-induced AhR activation has been extensively studied for many years, culminating in the commonly accepted model of a multistep process including 1) cytoplasmic to nuclear translocation, 2) shedding of Hsp90 and other chaperone proteins (presumably in the nucleus), 3) dimerizing with partner protein Arnt, and 4) transcription initiation mediated by AhR/Arnt heterodimer recruitment at target XRE enhancer sites. In addition, breaking of cell-cell contact or switching of cells from adherent culture to suspension also activates AhR (Sadek and Allen-Hoffmann, 1994; Cho et al., 2004; Ikuta et al., 2004). It has been suggested that activation of AhR by suspension shares many characteristics with typical ligand-induced AhR activation, including Hsp90 shedding, dimerization with partner protein Arnt, and proteasome-mediated AhR degradation (Cho et al., 2004). Thus, it was postulated that the mechanism of suspension-dependent AhR activation is very similar to that elicited by xenobiotics. Our data support this view, and we further showed that both xenobiotics and switching cells from adherent to suspension culture led to AhR recruitment to the same XRE enhancer sites of the prototypical endogenous target genes *Cyp1a1* and *Cyp1b1* and the more recently defined target gene *Tiparp* (Figs. 4 and 7). However, the suspension-dependent AhR recruitment showed lower efficacy than that induced by ligand, which agrees with previous reports that activation of AhR by suspension culture is more transient than that induced by xenobiotics (Monk et al., 2001; Cho et al., 2004).

Microarray experiments suggest that not all AhR target genes respond to xenobiotics in the same way as AhR activation invoked by switching cells from adherent culture to suspension. Of note, there are subsets of target genes that are regulated predominantly by xenobiotics, and there are also genes that are regulated predominantly by endogenous signaling-activated AhR (Fig. 2B). How the same signal transduction mechanism driven by both xenobiotics and endogenous signaling is able to activate AhR, resulting in transcriptional diversity specific to the type of initiating stimulus, is unclear. One possibility is that AhR is regulated through post-translational modification (PTM) much the same way as proposed for histones in the "histone code hypothesis." Different sets of post-translational modifications could be imposed on AhR, depending on the routes of its activation, resulting in restricted expression of specific target gene subsets that are sensitive to these particular modifications. PTM-dependent differential gene regulation has been shown to occur with other sequence-specific transcription factors such as tumor suppressor protein p53 and nuclear retinoic acid receptors (for reviews, see Knights et al., 2006; Rochette-Egly and Germain, 2009). Studies by our own laboratory also show that the AhR is heavily modified even in its latent state (K. A. Dave, S. G. B. Furness, H. Goswami, F. Whelan, C. Bindloss, N. Hao, M. L. Whitelaw, and J. J. Gorman, manuscript in preparation), which makes it a key candidate for PTM-dependent regulation. Thus, the combinatorial PTM patterns of AhR, especially those that are lost or newly acquired after xenobiotic exposure or in response to endogenous signaling, may lead to the differential recruitment of transcriptional coregulators to in turn modulate the expression of distinct subsets of AhR target genes. Consistent with this notion, the AhR has been shown to interact with a large number of transcription coactivators, including the p160 family of transcriptional coactivators NCoA-1/SRC-1 (nuclear receptor coactivator 1/steroid receptor coactivator-1), CBP (cAMP response element-binding protein-binding protein)/p300, RIP140 (receptor interacting protein 140), CoCoA (coiled-coil coactivator), and GAC63 (GRIP1 associated coactivator 63) (Beischlag et al., 2008).

Time course experiments also indicate that the temporal expression pattern of AhR target genes can vary widely (Fig. 3). Expression of *Serpinb2*, *Spint1*, and *GTRAP3-18* was rapidly up-regulated after AhR activation by ligand or suspension culture. However, at longer time points (8 h), the expression of these genes was restored back to basal levels. In contrast, the expression of *Cyp1a1*, *Cyp1b1*, and *Nqo1* was sustained at high levels across all time points upon AhR activation. This difference in the temporal expression pattern of AhR target genes may be due to variable mechanisms of AhR regulation on different promoters. Short-term induction followed by decline may reflect the need for the continued presence of the AhR, which is prevented by AhR turnover. At other promoters, the AhR may function primarily as a "pioneer factor," recruiting epigenetic modulators that clear repressive chromatin marks before the assembly of other transcription factors at the promoter that substitute for AhR in sustaining gene expression. Evidence for the latter exists for the mouse *Cyp1a1* gene, which is maintained in a nucleosomal conformation in its rest state that is relatively inaccessible for DNA-binding proteins. Activation of AhR increases the promoter occupancy of *Cyp1a1* whereby the level of *Cyp1a1* transcription correlates directly with the

load of general transcription factors such as Sp1, TBP, and NF1 at the *Cyp1a1* promoter (Kobayashi et al., 1996; Ko et al., 1997).

In this study, we provide evidence that *ApoER2* is a novel class II AhR target gene that is regulated predominantly by endogenous AhR activation (Table 1; Fig. 3). ApoER2 is a high-affinity Reelin receptor involved in memory formation and is implicated in modulating synaptic plasticity (Beffert et al., 2005), potentially linking to the physiological function of AhR. Of note, the ancestors of the mammalian AhR that are the invertebrate AhR orthologs such as *ahr-1* in *Caenorhabditis elegans* and *spineless* in *Drosophila* all have well established roles in neuronal development and morphogenesis (McMillan and Bradfield, 2007b).

The *GTRAP3-18* (glutamate transport-associated protein for EAAC1) gene was also identified as a novel AhR target in the microarray studies. However, in contrast to *ApoER2*, *GTRAP3-18* is a class III AhR target gene that is regulated by both xenobiotics and switching cells from adherent to suspension culture (Table 1; Fig. 3). GTRAP3-18 is a membrane-associated protein that negatively modulates intracellular glutathione levels (Watabe et al., 2008). Because glutathione protects neurons against oxidative stress-dependent neurodegenerative disease, xenobiotic-induced *GTRAP3-18* expression, which reduces intracellular glutathione levels, may contribute to neurotoxicity observed during xenobiotic-induced AhR activation (Williamson et al., 2005).

The mechanism of TCDD-induced toxicity represents one of the biggest questions in the AhR field. Despite years of research, how TCDD and related HAHs lead to toxic outcomes is still poorly understood. It is clear that TCDD-induced toxicity is AhR-dependent, because mice expressing a low-affinity AhR allele are partially resistant to TCDD and AhR-null mice are refractory to TCDD-induced teratogenicity (Okey et al., 1989; Mimura et al., 1997). However, the key genes responsible for the observed toxicological endpoints have not been convincingly identified. Part of the problem that limits our understanding of HAH-mediated toxicity may be due to the scope of most AhR studies. Much of the current research in the AhR field is protein-centric because microarray probes are often designed preferentially against protein coding transcripts. However, the contribution of ncRNAs toward TCDD-induced toxicity remains to be addressed. In this article, we showed for the first time that AhR coordinates the regulation of both the protein coding *Tiparp* gene and its *cis*-antisense ncRNA expression (Fig. 6), presumably via the same XRE enhancer element. Similar "head-to-head" arrangements also occur with the classic AhR target genes *Cyp1a1* and *Cyp1a2*, which are in close proximity (~4 kb apart) in the genome although they are transcribed in opposite orientations. Of interest, a recent study demonstrated that the adaptive *Cyp1a1*/*Cyp1a2* induction is also coregulated by a single XRE cluster spanning a 1.4-kb region upstream of the mouse *Cyp1a1* gene (Nukaya et al., 2009). With recent advances in sequencing technologies and better annotation of human and mouse genomes, it is likely that more examples of AhR regulatory hotspots that govern the induction of multiple genes within the same genomic loci may emerge. In fact, it has been estimated that ~40% of all human and mouse transcriptional units reside in *cis*-antisense pairs, with the vast majority of them involving ncRNAs (Engström et al., 2006). Thus, it is possible that the TCDD-elicited toxicological effect may be more complex than initially anticipated and may involve the coordinated expression of both protein coding mRNAs and regulatory ncRNAs.

Functional XREs have been identified for a number of bona fide AhR target genes including *Cyp1a1*, *Cyp1b1*, *Nqo1*, *Aldh3a1*, *Ugt1a6*, and *GstYa*, all of which are present at the 5′ flanking region of their TSS (Dere et al., 2011 and references therein). In contrast, we showed that the XRE for the mouse *Tiparp* gene is located in the first intron ~1.2 kb downstream of the TSS (Fig. 7). This is to our knowledge the first report of a functional XRE enhancer in the intron region of an AhR target gene. Consistent with this result, genome-wide ChIP-on-chip experiments using TCDD- or 3-methylcholanthrene-treated T47D breast cancer cells have identified hundreds of potential AhR binding sites beyond conventionally defined gene loci (Ahmed et al., 2009; Pansoy et al., 2010). The XRE of *Tiparp* features a concatemer of XRE core sequences (Fig. 7A) that is shared by another AhR target gene, *Cyp2s1* (Rivera et al., 2007). Intriguingly, both *Tiparp* and *Cyp2s1* genes are hypoxia-inducible by the mechanism of HIF-1α recruitment at XRE concatemer sites. It will now be important to search for other genes that may be regulated in this manner and determine whether overlapping HREs form a more general bHLH/PAS stress response *cis* element to aid cells to adapt or recover from perturbation.

Acknowledgments

We thank A/Professor Simon Barry (Women's and Children's Health Research Institute, North Adelaide, South Australia) for use of lentiviral expression and packaging plasmids; Professor J. Pelletier (McGill University, Montreal, QC, Canada) for pML-6c-wt reporter plasmid; Professor Gary Perdew (Pennsylvania State University, University Park, PA) for the *AhR*(−/−) hepatocyte cell line, Prof. C. K. Shim, Seoul National University and Yuhan Research Institute (Korea) for the gift of YH439; and Zhipeng Qu (University of Adelaide, Adelaide, South Australia) for help with bioinformatics analysis. We are also grateful to Dr. Henry Yang (National University of Singapore, Singapore, Singapore) for the use of the cross-correlation method for microarray normalization and to Norazean Zaiden (National University of Singapore) for technical assistance.

Authorship Contributions

Participated in research design: Hao, Lee, Poellinger, and Whitelaw.

Conducted experiments: Hao, Lee, Furness, and Bosdotter.

Performed data analysis: Hao, Lee, Poellinger, and Whitelaw.

Wrote or contributed to the writing of the manuscript: Hao, Lee, and Whitelaw.

References

Adachi J, Mori Y, Matsui S, and Matsuda T (2004) Comparison of gene expression patterns between 2,3,7,8-tetrachlorodibenzo-*p*-dioxin and a natural arylhydrocarbon receptor ligand, indirubin. *Toxicol Sci* **80:**161–169.

Ahmed S, Valen E, Sandelin A, and Matthews J (2009) Dioxin increases the interaction between aryl hydrocarbon receptor and estrogen receptor α at human promoters. *Toxicol Sci* **111:**254–266.

Beffert U, Weeber EJ, Durudas A, Qiu S, Masiulis I, Sweatt JD, Li WP, Adelmann G, Frotscher M, Hammer RE, et al. (2005) Modulation of synaptic plasticity and memory by Reelin involves differential splicing of the lipoprotein receptor Apoer2. *Neuron* **47:**567–579.

Beischlag TV, Luis Morales J, Hollingshead BD, and Perdew GH (2008) The aryl hydrocarbon receptor complex and the control of gene expression. *Crit Rev Eukaryot Gene Expr* **18:**207–250.

Bock KW and Köhle C (2006) Ah receptor: dioxin-mediated toxic responses as hints to deregulated physiologic functions. *Biochem Pharmacol* **72:**393–404.

Boutros PC, Moffat ID, Franc MA, Tijet N, Tuomisto J, Pohjanvirta R, and Okey AB (2004) Dioxin-responsive AHRE-II gene battery: identification by phylogenetic footprinting. *Biochem Biophys Res Commun* **321:**707–715.

Cho YC, Zheng W, and Jefcoate CR (2004) Disruption of cell-cell contact maximally

but transiently activates AhR-mediated transcription in 10T1/2 fibroblasts. *Toxicol Appl Pharmacol* **199:**220–238.
Chua SW, Vijayakumar P, Nissom PM, Yam CY, Wong VV, and Yang H (2006) A novel normalization method for effective removal of systematic variation in microarray data. *Nucleic Acids Res* **34:**e38.
de Waard WJ, Aarts JM, Peijnenburg AA, Baykus H, Talsma E, Punt A, de Kok TM, van Schooten FJ, and Hoogenboom LA (2008) Gene expression profiling in Caco-2 human colon cells exposed to TCDD, benzo[*a*]pyrene, and natural Ah receptor agonists from cruciferous vegetables and citrus fruits. *Toxicol In Vitro* **22:**396–410.
Denison MS and Nagy SR (2003) Activation of the aryl hydrocarbon receptor by structurally diverse exogenous and endogenous chemicals. *Annu Rev Pharmacol Toxicol* **43:**309–334.
Denison MS, Soshilov AA, He G, DeGroot DE, and Zhao B (2011) Exactly the same but different: promiscuity and diversity in the molecular mechanisms of action of the aryl hydrocarbon (dioxin) receptor. *Toxicol Sci* **124:**1–22.
Dere E, Boverhof DR, Burgoon LD, and Zacharewski TR (2006) In vivo-in vitro toxicogenomic comparison of TCDD-elicited gene expression in Hepa1c1c7 mouse hepatoma cells and C57BL/6 hepatic tissue. *BMC Genomics* **7:**80.
Dere E, Forgacs AL, Zacharewski TR, and Burgoon LD (2011) Genome-wide computational analysis of dioxin response element location and distribution in the human, mouse, and rat genomes. *Chem Res Toxicol* **24:**494–504.
Diani-Moore S, Ram P, Li X, Mondal P, Youn DY, Sauve AA, and Rifkind AB (2010) Identification of the aryl hydrocarbon receptor target gene *TiPARP* as a mediator of suppression of hepatic gluconeogenesis by 2,3,7,8-tetrachlorodibenzo-*p*-dioxin and of nicotinamide as a corrective agent for this effect. *J Biol Chem* **285:**38801–38810.
Dinger ME, Amaral PP, Mercer TR, Pang KC, Bruce SJ, Gardiner BB, Askarian-Amiri ME, Ru K, Soldà G, Simons C, et al. (2008) Long noncoding RNAs in mouse embryonic stem cell pluripotency and differentiation. *Genome Res* **18:**1433–1445.
Dzeletovic N, McGuire J, Daujat M, Tholander J, Ema M, Fujii-Kuriyama Y, Bergman J, Maurel P, and Poellinger L (1997) Regulation of dioxin receptor function by omeprazole. *J Biol Chem* **272:**12705–12713.
Eisen MB, Spellman PT, Brown PO, and Botstein D (1998) Cluster analysis and display of genome-wide expression patterns. *Proc Natl Acad Sci USA* **95:**14863–14868.
Engström PG, Suzuki H, Ninomiya N, Akalin A, Sessa L, Lavorgna G, Brozzi A, Luzi L, Tan SL, Yang L, et al. (2006) Complex loci in human and mouse genomes. *PLoS Genet* **2:**e47.
Farrall AL and Whitelaw ML (2009) The HIF1α-inducible pro-cell death gene BNIP3 is a novel target of SIM2s repression through cross-talk on the hypoxia response element. *Oncogene* **28:**3671–3680.
Furness SG and Whelan F (2009) The pleiotropy of dioxin toxicity-xenobiotic misappropriation of the aryl hydrocarbon receptor's alternative physiological roles. *Pharmacol Ther* **124:**336–353.
Hao N, Whitelaw ML, Shearwin KE, Dodd IB, and Chapman-Smith A (2011) Identification of residues in the N-terminal PAS domains important for dimerization of Arnt and AhR. *Nucleic Acids Res* **39:**3695–3709.
Henry EC, Welle SL, and Gasiewicz TA (2010) TCDD and a putative endogenous AhR ligand, ITE, elicit the same immediate changes in gene expression in mouse lung fibroblasts. *Toxicol Sci* **114:**90–100.
Hestermann EV and Brown M (2003) Agonist and chemopreventative ligands induce differential transcriptional cofactor recruitment by aryl hydrocarbon receptor. *Mol Cell Biol* **23:**7920–7925.
Huang G and Elferink CJ (2012) A novel nonconsensus xenobiotic response element capable of mediating aryl hydrocarbon receptor-dependent gene expression. *Mol Pharmacol* **81:**338–347.
Ikuta T, Kobayashi Y, and Kawajiri K (2004) Cell density regulates intracellular localization of aryl hydrocarbon receptor. *J Biol Chem* **279:**19209–19216.
Kazlauskas A, Poellinger L, and Pongratz I (1999) Evidence that the co-chaperone p23 regulates ligand responsiveness of the dioxin (aryl hydrocarbon) receptor. *J Biol Chem* **274:**13519–13524.
Kim S, Dere E, Burgoon LD, Chang CC, and Zacharewski TR (2009) Comparative analysis of AhR-mediated TCDD-elicited gene expression in human liver adult stem cells. *Toxicol Sci* **112:**229–244.
Kiss EA, Vonarbourg C, Kopfmann S, Hobeika E, Finke D, Esser C, and Diefenbach A (2011) Natural aryl hydrocarbon receptor ligands control organogenesis of intestinal lymphoid follicles. *Science* **334:**1561–1565.
Knights CD, Catania J, Di Giovanni S, Muratoglu S, Perez R, Swartzbeck A, Quong AA, Zhang X, Beerman T, Pestell RG, et al. (2006) Distinct p53 acetylation cassettes differentially influence gene-expression patterns and cell fate. *J Cell Biol* **173:**533–544.
Ko HP, Okino ST, Ma Q, and Whitlock JP Jr (1997) Transactivation domains facilitate promoter occupancy for the dioxin-inducible CYP1A1 gene in vivo. *Mol Cell Biol* **17:**3497–3507.
Kobayashi A, Sogawa K, and Fujii-Kuriyama Y (1996) Cooperative interaction between AhR · Arnt and Sp1 for the drug-inducible expression of CYP1A1 gene. *J Biol Chem* **271:**12310–12316.
Lee IJ, Jeong KS, Roberts BJ, Kallarakal AT, Fernandez-Salguero P, Gonzalez FJ, and Song BJ (1996) Transcriptional induction of the cytochrome P4501A1 gene by a thiazolium compound, YH439. *Mol Pharmacol* **49:**980–988.
Li Y, Innocentin S, Withers DR, Roberts NA, Gallagher AR, Grigorieva EF, Wilhelm C, and Veldhoen M (2011) Exogenous stimuli maintain intraepithelial lymphocytes via aryl hydrocarbon receptor activation. *Cell* **147:**629–640.
Lusska A, Shen E, and Whitlock JP Jr (1993) Protein-DNA interactions at a dioxin-responsive enhancer. Analysis of six bona fide DNA-binding sites for the liganded Ah receptor. *J Biol Chem* **268:**6575–6580.
Marlowe JL, Knudsen ES, Schwemberger S, and Puga A (2004) The aryl hydrocarbon receptor displaces p300 from E2F-dependent promoters and represses S phase-specific gene expression. *J Biol Chem* **279:**29013–29022.
McMillan BJ and Bradfield CA (2007a) The aryl hydrocarbon receptor is activated by modified low-density lipoprotein. *Proc Natl Acad Sci USA* **104:**1412–1417.
McMillan BJ and Bradfield CA (2007b) The aryl hydrocarbon receptor sans xenobiotics: endogenous function in genetic model systems. *Mol Pharmacol* **72:**487–498.
Mimura J, Yamashita K, Nakamura K, Morita M, Takagi TN, Nakao K, Ema M, Sogawa K, Yasuda M, Katsuki M, et al. (1997) Loss of teratogenic response to 2,3,7,8-tetrachlorodibenzo-*p*-dioxin (TCDD) in mice lacking the Ah (dioxin) receptor. *Genes Cells* **2:**645–654.
Monk SA, Denison MS, and Rice RH (2001) Transient expression of CYP1A1 in rat epithelial cells cultured in suspension. *Arch Biochem Biophys* **393:**154–162.
Murray IA, Reen RK, Leathery N, Ramadoss P, Bonati L, Gonzalez FJ, Peters JM, and Perdew GH (2005) Evidence that ligand binding is a key determinant of Ah receptor-mediated transcriptional activity. *Arch Biochem Biophys* **442:**59–71.
Nukaya M, Moran S, and Bradfield CA (2009) The role of the dioxin-responsive element cluster between the Cyp1a1 and Cyp1a2 loci in aryl hydrocarbon receptor biology. *Proc Natl Acad Sci USA* **106:**4923–4928.
Okey AB, Vella LM, and Harper PA (1989) Detection and characterization of a low affinity form of cytosolic Ah receptor in livers of mice nonresponsive to induction of cytochrome P1-450 by 3-methylcholanthrene. *Mol Pharmacol* **35:**823–830.
Pansoy A, Ahmed S, Valen E, Sandelin A, and Matthews J (2010) 3-Methylcholanthrene induces differential recruitment of aryl hydrocarbon receptor to human promoters. *Toxicol Sci* **117:**90–100.
Patel RD, Murray IA, Flaveny CA, Kusnadi A, and Perdew GH (2009) Ah receptor represses acute-phase response gene expression without binding to its cognate response element. *Lab Invest* **89:**695–707.
Rivera SP, Wang F, Saarikoski ST, Taylor RT, Chapman B, Zhang R, and Hankinson O (2007) A novel promoter element containing multiple overlapping xenobiotic and hypoxia response elements mediates induction of cytochrome P4502S1 by both dioxin and hypoxia. *J Biol Chem* **282:**10881–10893.
Rochette-Egly C and Germain P (2009) Dynamic and combinatorial control of gene expression by nuclear retinoic acid receptors (RARs). *Nucl Recept Signal* **7:**e005.
Sadek CM and Allen-Hoffmann BL (1994) Suspension-mediated induction of Hepa 1c1c7 Cyp1a-1 expression is dependent on the Ah receptor signal transduction pathway. *J Biol Chem* **269:**31505–31509.
Sogawa K, Numayama-Tsuruta K, Takahashi T, Matsushita N, Miura C, Nikawa J, Gotoh O, Kikuchi Y, and Fujii-Kuriyama Y (2004) A novel induction mechanism of the rat CYP1A2 gene mediated by Ah receptor-Arnt heterodimer. *Biochem Biophys Res Commun* **318:**746–755.
Stevens EA, Mezrich JD, and Bradfield CA (2009) The aryl hydrocarbon receptor: a perspective on potential roles in the immune system. *Immunology* **127:**299–311.
Tijet N, Boutros PC, Moffat ID, Okey AB, Tuomisto J, and Pohjanvirta R (2006) Aryl hydrocarbon receptor regulates distinct dioxin-dependent and dioxin-independent gene batteries. *Mol Pharmacol* **69:**140–153.
Watabe M, Aoyama K, and Nakaki T (2008) A dominant role of GTRAP3-18 in neuronal glutathione synthesis. *J Neurosci* **28:**9404–9413.
Whelan F, Hao N, Furness SG, Whitelaw ML, and Chapman-Smith A (2010) Amino acid substitutions in the aryl hydrocarbon receptor ligand binding domain reveal YH439 as an atypical AhR activator. *Mol Pharmacol* **77:**1037–1046.
Williamson MA, Gasiewicz TA, and Opanashuk LA (2005) Aryl hydrocarbon receptor expression and activity in cerebellar granule neuroblasts: implications for development and dioxin neurotoxicity. *Toxicol Sci* **83:**340–348.
Wu TD and Nacu S (2010) Fast and SNP-tolerant detection of complex variants and splicing in short reads. *Bioinformatics* **26:**873–881.

Address correspondence to: A/Prof. Murray Whitelaw, School of Molecular and Biomedical Science (Biochemistry), The University of Adelaide, North Tce, Adelaide, SA 5005, Australia. E-mail: murray.whitelaw@adelaide.edu.au